



## Letter

**Cite this article:** Diaz MA, Gardner CB, Elliot DH, Adams BJ, Lyons WB (2023). Change at 85 degrees south: Shackleton Glacier region proglacial lakes from 1960 to 2020. *Annals of Glaciology* 64(92), 181–186. <https://doi.org/10.1017/aog.2023.27>

Received: 28 December 2022

Revised: 25 February 2023

Accepted: 10 March 2023

First published online: 5 May 2023

**Key words:**


Antarctic glaciology; climate change; meltwater chemistry

**Corresponding author:**

Melisa A. Diaz,

E-mail: [melisa.diaz@colorado.edu](mailto:melisa.diaz@colorado.edu)

# Change at 85 degrees south: Shackleton Glacier region proglacial lakes from 1960 to 2020

Melisa A. Diaz<sup>1,2</sup> , Christopher B. Gardner<sup>1</sup>, David H. Elliot<sup>1</sup>, Byron J. Adams<sup>3,4</sup> and W. Berry Lyons<sup>1</sup>

<sup>1</sup>School of Earth Sciences and Byrd Polar and Climate Research Center, The Ohio State University, Columbus, Ohio, USA; <sup>2</sup>Department of Geography and Institute of Arctic and Alpine Research, University of Colorado Boulder, Boulder, Colorado, USA; <sup>3</sup>Department of Biology and Evolutionary Ecology Laboratories, Brigham Young University, Provo, Utah, USA and <sup>4</sup>Monte L. Bean Life Science Museum, Brigham Young University, Provo, Utah, USA

**Abstract**

Over the last two decades, anomalous warming events have been observed in coastal Antarctic regions. While these events have been documented in the Ross Sea sector, the Antarctic interior is believed to have been buffered from warming. In this work, we present data from lakes located near Mt. Heekin and Thanksgiving Valley (~85° S) along the Shackleton Glacier, which are believed to be the southern-most Antarctic dry valley lakes. In 2018, the lakes were characterized, repeat satellite images were examined, and lake water chemistry was measured. Our analysis shows that lake areas recently increased, and the water-soluble ion chemistry indicates a flushing of salts from periglacial soils, likely from increased glacial melt as illustrated by water isotope data. Our results show that high southern latitude ice-free areas have likely been affected by warm pulses over the past 60 years and these pulses may be quasi-synchronous throughout the Transantarctic Mountains.

**Introduction**

The Antarctic Ice Sheet is losing ice at an accelerated rate and has contributed  $7.6 \pm 3.9$  mm to global sea level rise between 1992 and 2017 (Shepherd and others, 2018). Much of the mass loss from Antarctica has occurred via ice sheet thinning at glacial margins and calving events on ice shelves (e.g., Greene and others, 2022). These calving events are believed to be influenced by supraglacial melt. Recent work has identified and mapped over 65 000 supraglacial lakes along the margin of the East Antarctic Ice Sheet (EAIS), some of which can induce hydro-fracturing near grounding lines (Stokes and others, 2019). While the occurrence and variability of supraglacial meltwater is largely believed to be due to synoptic scale climatological patterns (Donat-Magnin and others, 2020), little is documented about modern warming events and meltwater storage for the Transantarctic Mountains (TAM).

Evidence of warming and increased meltwater production has been documented at lower latitudes along the TAM. For example, a cooling trend observed 1986–2001 ended in the McMurdo Dry Valleys (~77.6° S) with a ‘flood year’ during the austral summer of 2001–2002 (Barrett and others, 2008; Gooseff and others, 2017). Enhanced melt of alpine and piedmont glaciers resulted in substantive increases in stream flow and lake level rise, which freshened the hypolimnion of the lakes and effectively ‘reset’ a decade of cryoconcentration (Barrett and others, 2008). This flood year was the start of a regime shift toward elevated summer meltwater generation, lake ice thinning, and changes in ecosystem structure that have persisted for over a decade (Gooseff and others, 2017). Farther south (~250 km) along the Darwin Glacier, lake levels for proglacial Lake Wilson increased by 20 m between 1975 and 1993 (Webster and others, 1996). The flux of meltwater adversely affected lake biological communities, with primary production limited to the upper mixed layer (Webster and others, 1996). Lake Wilson was believed to be the southernmost dry valley lake, until the Shackleton Glacier region lakes were identified and described (Elliot and others, 1996; Dengler, 2013). In this work, we provide both imagery and geochemical evidence for a dynamic hydrologic system in high elevation, high southern latitude dry valleys. Our goal was not a comprehensive analysis of all high southern latitude lakes, but instead to focus on two previously identified systems for which remote sensing and in situ data could be interpreted, and to provide recommendations for future work.

**Study site**

The Shackleton Glacier is a major outlet glacier of the EAIS and flows ~130 km south to north through the Queen Maud Mountains of the Central Transantarctic Mountains. To the south, east, and west of the glacier, dry valleys are present among the mountain peaks. Two of these valleys are the focus of this work: colloquially known as Thanksgiving Valley and Heekin Valley (Fig. 1).

Thanksgiving Valley (–84.9164, –177.0218) is located near the intersection of Shackleton Glacier and Mincey Glacier, a smaller tributary. Rogue and Butters glaciers also flow into the

© The Author(s), 2023. Published by Cambridge University Press on behalf of International Glaciological Society. This is an Open Access article, distributed under the terms of the Creative Commons Attribution licence (<http://creativecommons.org/licenses/by/4.0/>), which permits unrestricted re-use, distribution and reproduction, provided the original article is properly cited.

[cambridge.org/aog](https://www.cambridge.org/aog)



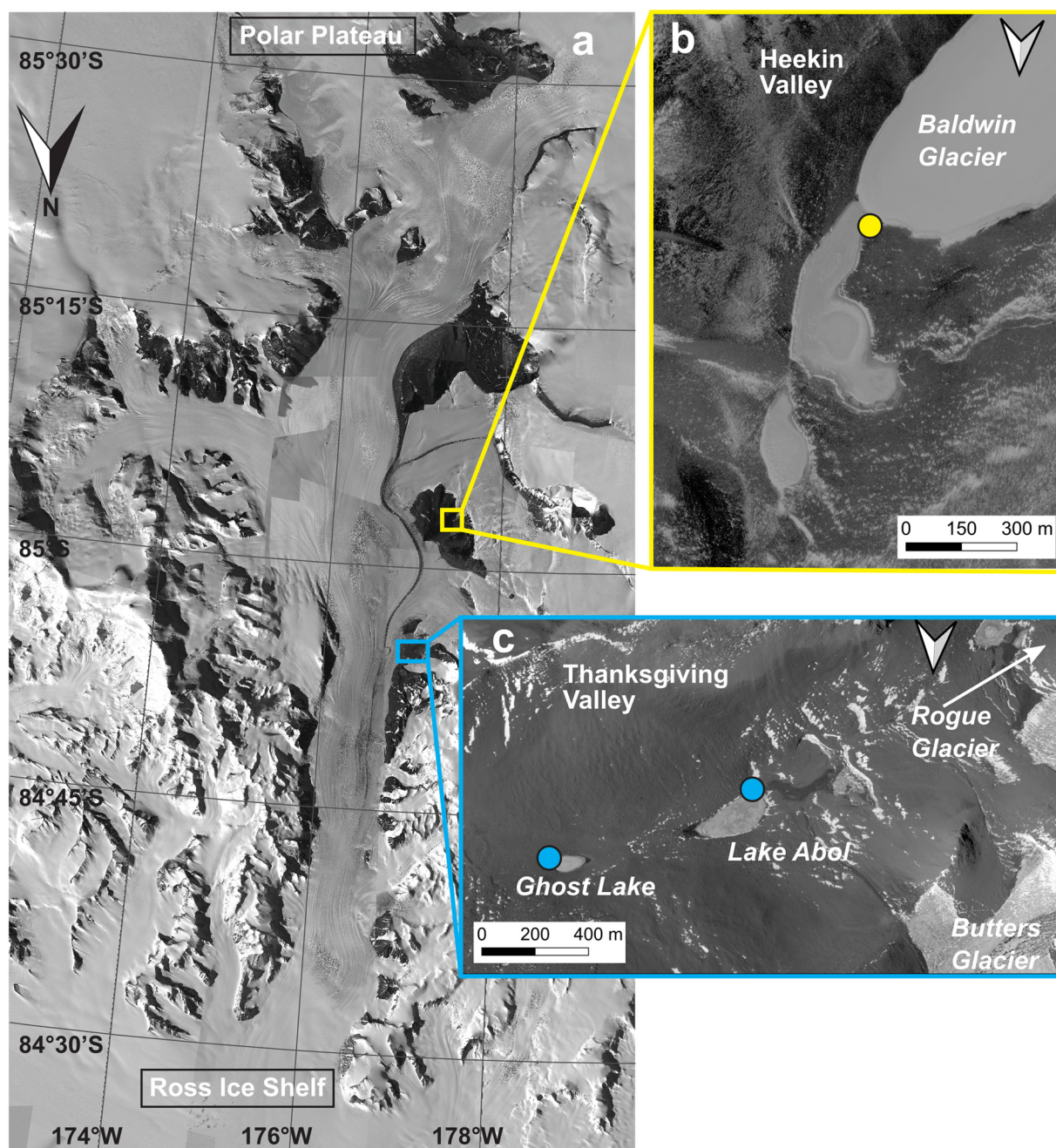


**Figure 1.** Sampling locations of lakes near Mt. Heekin ('Heekin Valley') and Thanksgiving Valley along the Shackleton Glacier, Antarctica. The locations for water sampling are noted in each inset. All images are visible panchromatic WorldView-1, -2, and -3 images acquired with assistance from the Polar Geospatial Center.

valley and can contribute to glacial runoff. Thanksgiving Valley is nearly perpendicular to Shackleton Glacier and trends SW-NE, at about 3.5 km length and 1.5 km width and has ridges to the north and south. Six ponds and lakes have been noted in the valley: Thanksgiving Lake – the largest, Bald Pond – the smallest, Speckled Pond, Baxter Pond, Lake Abol, and Ghost Lake (see Dengler, 2013). Lake Abol and Ghost Lake are in the deepest portion of the valley and are separated from Shackleton Glacier by a large saddle. Dengler (2013) noted that Lake Abol is fed by meltwater from Butters Glacier and a local snowpack. It occasionally spills over and feeds Ghost Lake. Algal samples taken near Ghost Lake had radiocarbon ages of approximately 10 ka and the meteoric  $^{10}\text{Be}$  estimated exposure duration near Lake Abol suggests that the surface has an exposure duration of approximately 250 ka (Dengler, 2013; Diaz and others, 2021b).

Mt. Heekin is located near the intersection of Baldwin and Shackleton glaciers. A large saddle separates a deep valley,

informally termed 'Heekin Valley', from Mincey Glacier. Meltwater from a tongue of Baldwin Glacier and higher elevation snowpack pools at the valley floor to form a dry-valley lake that occasionally spills over to form lakes at slightly lower elevations. Elliot and others (1996) identified modern algal mats near the Heekin lakes and mats near Shackleton Glacier were later dated to a maximum of approximately 3000 yrs (Dengler, 2013). The lakes at Mount Heekin are located about 990 m a.s.l. and the lakes at Thanksgiving are at approximately 1080 m a.s.l., which is significantly higher elevation than the McMurdo Dry Valleys lakes which are less than 50 m a.s.l.

### Methods

Water samples were collected from melted lake moats at both Lake Abol and Ghost Lake. Samples were collected for ions and nutrients ( $\text{Na}^+$ ,  $\text{K}^+$ ,  $\text{Ca}^{2+}$ ,  $\text{Mg}^{2+}$ ,  $\text{Cl}^-$ ,  $\text{PO}_4^{3-}$ ,  $\text{NO}_3^- + \text{NO}_2^-$  and



NH<sub>3</sub>), and stable water isotopes ( $\delta^{18}\text{O}$  and  $\delta^2\text{H}$ ). All samples were filtered immediately upon collection using a clean plastic syringe and passed through a 0.45  $\mu\text{m}$  nylon syringe filter. The ion and nutrient samples were frozen upon return to Shackleton camp (within three hours). The water isotope samples were filled and capped with no headspace and kept chilled ( $\sim+4^\circ\text{C}$ ) until analysis.

The aqueous geochemistry analytical techniques used here are similar to those reported by Diaz and others (2021a) and Welch and others (2010). In summary, the cations were measured on a PerkinElmer Optima 8300 Inductively Coupled Plasma-Optical Emission Spectrometer (ICP-OES), anions on a Dionex ICS-2100 ion chromatograph, nutrients on a Skalar San++ Automated Wet Chemistry Analyzer, and water isotopes on a Picarro Wavelength Scanned-Cavity Ring Down Spectroscopy Analyzer Model L1102-I at The Ohio State University. Accuracy was typically better than 5%, as determined by the NIST 1643e external reference standard and the 2015 USGS interlaboratory calibration standard (M-216).  $\delta^{18}\text{O}$  and  $\delta^2\text{H}$  measurements are reported with respect to Vienna Standard Mean Ocean Water.

Satellite images were collected with the assistance of the Polar Geospatial Center and included a variety of satellite products, namely visible panchromatic WorldView-1, -2, and -3. No georeferenced images could be analyzed prior to 2009 for either valley due to the high occurrence of clouds and gaps in data. Additionally, deep shadows at the valley floors during summertime eliminate the possibility of using digital elevation models to estimate depth, and subsequently volume, of the lakes in Thanksgiving and Heekin Valleys. Images were processed via

ESRI ArcGIS Pro 2.1 and areas were measured by hand by creating polygons using internal applications.

## Results and discussion

### Heekin Valley lakes

In 1996, three small ponds were identified and sampled in Heekin Valley: one in contact with the glacial tongue ( $\sim 700\text{ m}^2$ ), and two isolated ponds on the valley floor further away ( $\sim 9700\text{ m}^2$  and  $\sim 17\,500\text{ m}^2$ ) (Elliot and others, 1996). Elliot and others (1996) also identified a dried pond bed near one of the isolated ponds (Fig. 2b). An archived image flyover near Mt. Heekin in 1960 indicates that the ponds in Heekin Valley had not drastically changed in area when the ponds were sampled in 1996 (Elliot and others, 1996), suggesting that this environment may have been essentially static for approximately 40 years, though lake levels were certainly higher in the more distant past (Dengler, 2013; Diaz and others, 2021b). We visited the site again a decade later in December 2007. Aerial images show that the original three ponds and the dry pond bed had filled and merged into a single large lake (Fig. 2c). When we visited the site approximately another decade later, a second, subsidiary lake had formed due to spillover of the first, primary lake. We observed later stages of the subsidiary lake formation in satellite imagery. The subsidiary lake had begun forming sometime after 2007 but prior to 2009. Between 2009 and 2018, water can be seen in a stream flowing over a ridge to feed the subsidiary lake, which increased in area from approximately  $11\,500\text{ m}^2$  to  $21\,300\text{ m}^2$  over this time

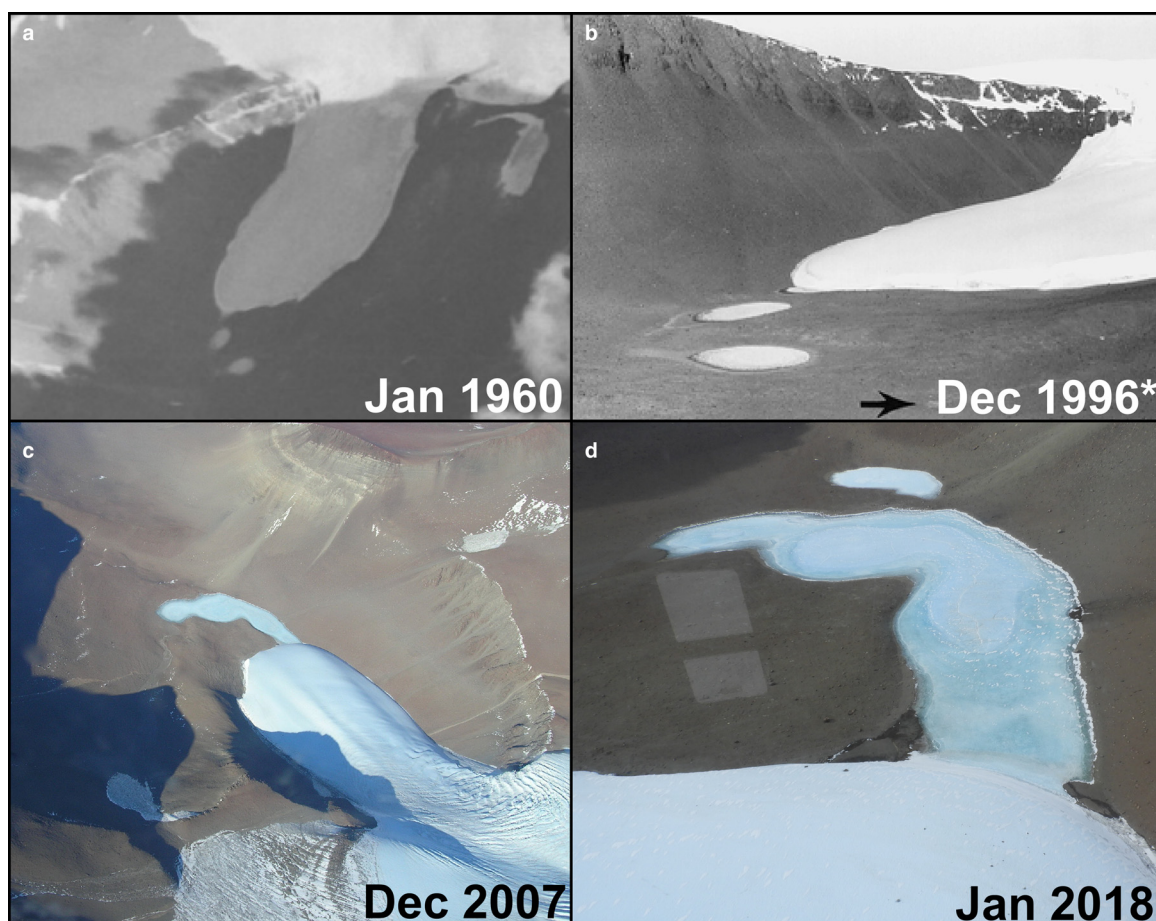


**Figure 2.** Timeseries of the Mt. Heekin ponds and lakes from 1960 to 2017. The aerial image (TMA 786 33R 0052) in (a) and ground image in (b) show the three separate ponds (oriented south), while (c) and (d) are aerial images showing that the original ponds merged and a subsidiary lake formed (oriented north). The 1996 image (b) is from Elliot and others (1996), with the black arrow indicating a dried pond bed.

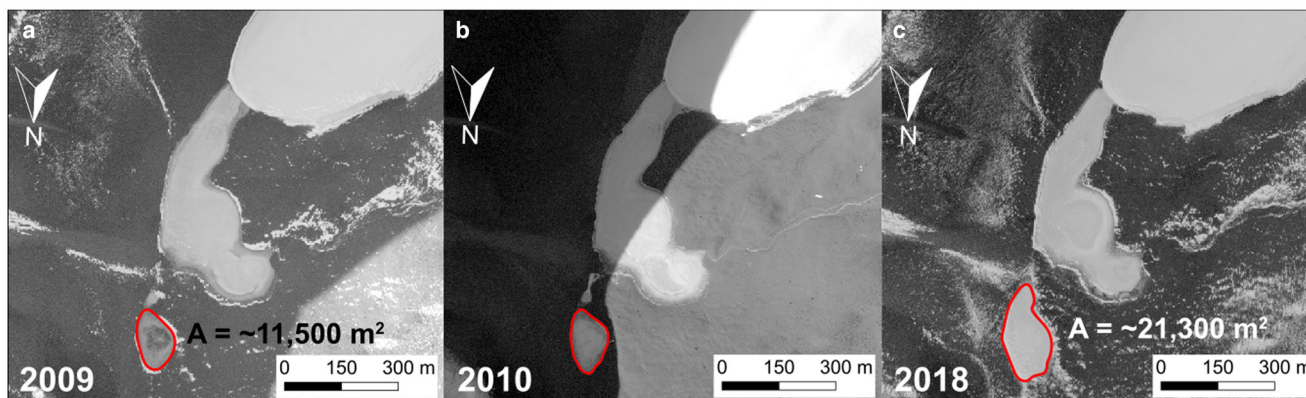


Figure 3. Growth of the subsidiary Heekin Valley lake, as shown by satellite images from PGC.

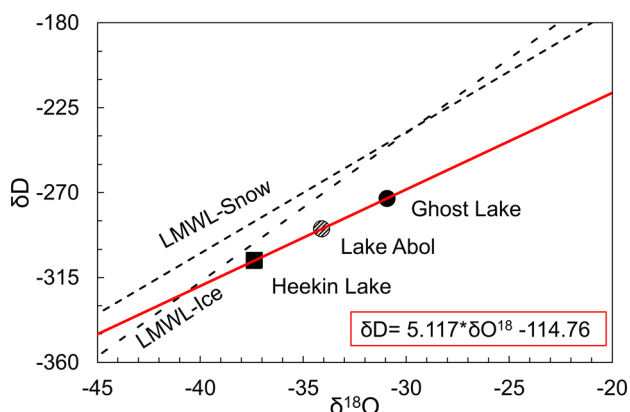


Figure 4. Water stable isotopes of the Heekin and Thanksgiving valley lakes. The local meteoric water lines, calculated from published data (Helsen and others, 2007; Masson-Delmotte and others, 2008), for ice and snow are shown.

(Fig. 3). Water can also be seen in a stream filling the primary lake from the glacier tongue and from a small stream draining glacial ice and snowpack higher up along the valley wall.

These observations are validated by water stable isotope measurements from the primary and largest lake. When  $\delta^{18}\text{O}$  and  $\delta^2\text{H}$  were plotted along with generalized local meteoric water lines (calculated from published data (Helsen and others, 2007; Masson-Delmotte and others, 2008)) for both ice and snow, the Heekin lake values suggest that the majority of water is derived from glacial melt that has been ponded and then evaporated (Fig. 4). In terms of the water-soluble salt and nutrient geochemistry, concentrations of  $\text{PO}_4^{3-}$  decreased from the three-lake average of  $\sim 0.31 \mu\text{M}$  to  $0.10 \mu\text{M}$  from 1996 to 2018 (Table 1).  $\text{NO}_3^-$  values increased, which is unsurprising given the high concentrations of nitrate salts in the region sourced from atmospheric deposition (Diaz and others, 2021a, 2020).

### Thanksgiving Valley lakes

Higher temporal resolution images were analyzed for Thanksgiving Valley compared to Heekin Valley, as we were

able to attain nearly yearly and sometimes sub-annual resolution images to understand the lake filling and drainage mechanisms from 2009 to 2020. Lake Abol does not significantly change in size until it overfills and spills into Ghost Lake. In 2009 and 2010, Ghost Lake was completely dry but filled by the time the next image was taken in 2013. From 2014 to 2020, the lake slowly decreased in area until 2018, when it filled again and then evaporates (Fig. 5). Lake Abol receives most of its water from Butters and Rogue glaciers, as evidenced by the stable water isotope composition; the water is glacially sourced and evaporated.

The water-soluble ion concentrations for the Abol and Ghost lakes are comparable with those from Heekin. However, Ghost generally has the highest concentrations of conservative ions and, in particular, has approximately twice the amount of sodium and chloride as Abol, which is expected given that the lake was evaporating in 2018. Concentrations of  $\text{PO}_4^{3-}$  were below the analytical detection limit for Ghost Lake and ammonia concentrations were the highest. Any P entering these lakes is derived from the chemical weathering of the soils as the glacial meltwaters flow over and through them, as the soils in the region have not been wetted previously for several thousand years (Diaz and others, 2021b). This P is consumed via algal growth, thus lowering its concentration below our analytical detection limit. The system is likely P limited (Barrett and others, 2007), where even bioavailable N (e.g., ammonia) could accumulate. We did not observe any algal mat, though Dengler (2013) noted dried mats along paleo-lake shores. No analysis has been done to determine the microbial composition in any of these lakes, but our preliminary work yielded no diatom counts.

### Quasi-synchronous widespread melting

We compared the timing of lake filling for Heekin and Thanksgiving valleys with flow records from the Onyx River in the McMurdo Dry Valleys  $\sim 1000 \text{ km NW}$  (Fig. 6). The Onyx River has the longest flow record of dry valley streams, dating back to 1970, and can be used as a sentinel for hydrologic changes (Gooseff and others, 2007). Our comparison indicates that during the period from 1975 to 1993 when Lake Wilson

Table 1. Water-soluble ion concentrations from the Heekin and Thanksgiving (TGV) valley lakes (this study, 2018) and the data reported by Elliot and others (1996) from Mt. Heekin

	Latitude	Longitude	Na ( $\mu\text{M}$ )	Mg ( $\mu\text{M}$ )	K ( $\mu\text{M}$ )	Ca ( $\mu\text{M}$ )	$\text{PO}_4$ ( $\mu\text{M}$ )	$\text{NO}_3 + \text{NO}_2$ ( $\mu\text{M}$ )	$\text{NH}_3$ ( $\mu\text{M}$ )	Cl ( $\mu\text{M}$ )
Ghost Lake	-84.9164	-177.0218	825	191	20.0	195	BDL	202	31.6	880
Lake Abol	-84.9150	-176.9069	403	126	19.4	108	0.082	257	5.31	350
Heekin	-85.0528	-177.4099	487	108	13.3	213	0.100	217	3.57	307
Elliot and others (1996)	-85.0528	-177.4099	364	49.2	7.93	116	0.313	63.7	9.32	-

BDL represents data below detection limit.

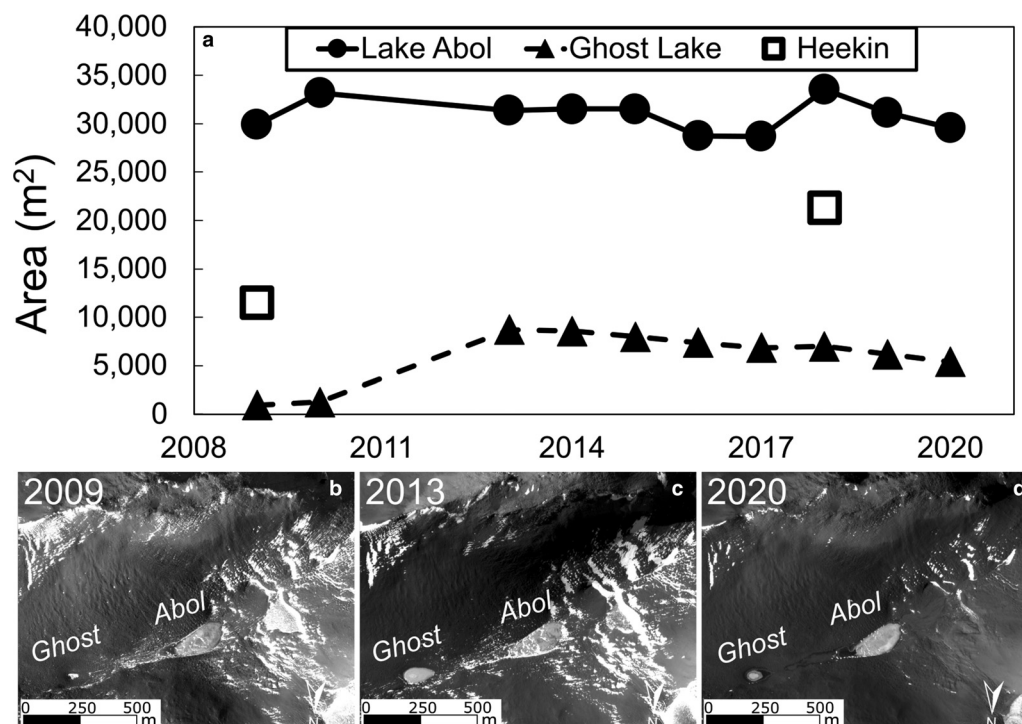


**Figure 5.** Timeseries of the Thanksgiving Valley lakes from 2009 to 2020 (a). The subsidiary Heekin lake is plotted for comparison. Aerial images showing the disappearance (b), growth (c), and evaporation (d) of Ghost Lake.

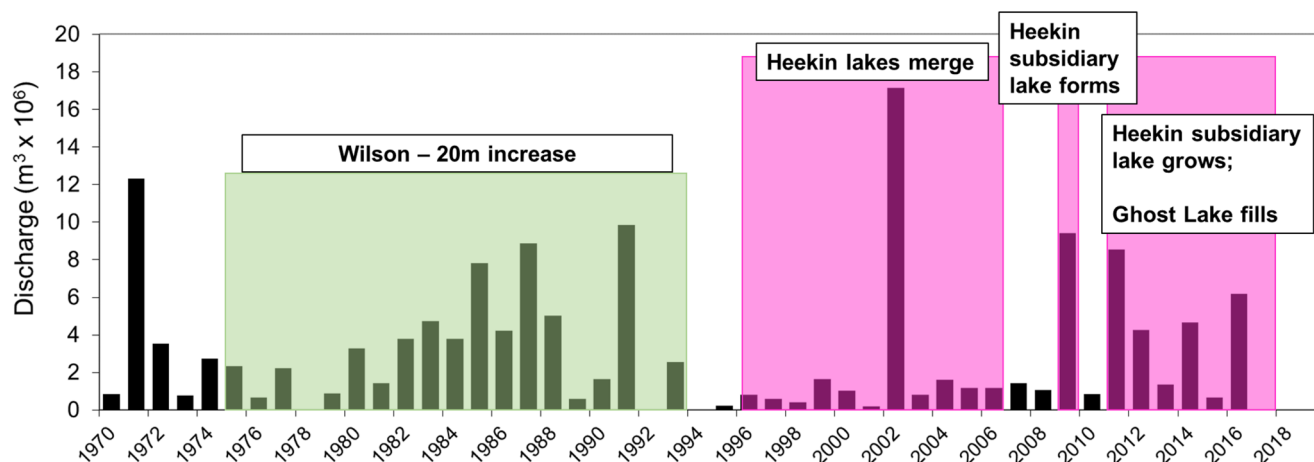


**Figure 6.** Timing of lake growth and formation in the Central Transantarctic Mountains in the context of flow (discharge) from the Onyx River in the McMurdo Dry Valleys. Flow data were compiled from the McMurdo LTER (DOI: 10.6073/pasta/4370a8c48ad3b1f5f1de7aa43155e13c).

deepened by 20 m, there were some smaller pulses of meltwater flow for the Onyx. The Heekin lakes merged between 1996 and 2006, during which the flood year in the McMurdo Dry Valleys occurred (2002). There was another meltwater pulse in the Onyx record in 2009, which coincided with the formation of the subsidiary lake in Heekin Valley, and the elevated river flow from 2012–2018 was during a period when Ghost Lake filled and the subsidiary Heekin lake grew. While rudimentary, our comparison of these records suggests that increased glacier meltwater generation was quasi-synchronous between the McMurdo Dry Valleys and the Central Transantarctic Mountains. In other words, regional warming and concomitant hydrological changes in the Central Transantarctic Mountains might be more widespread and dynamic than previously thought (Jones and others, 2019).

## Conclusions and recommendations

No data from long-term weather stations are available in the TAM and studies on the influence of summer temperature variations and the potential generation of surface meltwater in East Antarctica are limited to coastal regions (e.g., Stokes and others, 2019). As a result, the hydrologic system in the Central Transantarctic Mountains is thought to be fairly static and evidence of active meltwater generation has been anecdotal (Bell and others, 2018). In this study, we analyzed two lake systems in the Shackleton Glacier region which, to our knowledge, are the southernmost dry valley lakes. However, we speculate that there are additional lakes in the Central Transantarctic Mountains that have yet to be formally documented.

Satellite imagery and aerial photographs show that the lakes in Heekin Valley have grown in size and merged, filling a previously



dry pond bed, and the lakes in Thanksgiving Valley have grown, evaporated, and overflowed through the last 30 years. The water is primarily derived from glacial melt, and the water-soluble ion geochemistry suggests that the lakes may have active modern biological communities. Documented pulses of glacial meltwater in the Shackleton Glacier region appear to coincide with long-term climate warming and meltwater pulses 1000 km away in the McMurdo Dry Valleys. It is possible warming trends are widespread throughout the TAM and dry valleys can provide evidence for past and current meltwater storage.

These high elevation, high southern latitude lakes may be our only indicators of warming and glacier melting near the Antarctic interior, yet they are understudied. Our data may be used to verify Climate Reanalysis datasets (Carter and others, 2022). Additional studies are needed focusing both on remote sensing: to identify and characterize additional meltwater lakes at high southern latitudes, quantify rates of glacier melting, and infer weather and climatic changes, and in situ analysis: to understand the sources of meltwater generation and mechanisms of alteration, rates of chemical weathering, and changes in soil and lake habitability.

**Acknowledgements.** We thank the United States Antarctic Program (USAP), Antarctic Science Contractors (ASC), and Petroleum Helicopters Inc. (PHI) for logistical and field support. We are especially grateful to Michael Cloutier (PGC) for his help in acquiring satellite imagery from the Shackleton Glacier region, S. Welch for help with the geochemical measurements, and D. Smith for help with the water isotope measurements. Geospatial support for this work was provided by the Polar Geospatial Center under NSF-OPP awards 1043681 and 1559691. This work was supported by NSF-OPP awards 1341631 and 1341629 to WBL and BJA, and NSF-GRFP 60041697 awarded to MAD.

## References

- Barrett JE and 8 others** (2007) Biogeochemical stoichiometry of Antarctic Dry Valley ecosystems. *Journal of Geophysical Research* **112**(G1), G01010. doi: [10.1029/2005JG000141](https://doi.org/10.1029/2005JG000141).
- Barrett JE and 6 others** (2008) Persistent effects of a discrete warming event on a polar desert ecosystem. *Global Change Biology* **14**, 2249–2261. doi: [10.1111/j.1365-2486.2008.01641.x](https://doi.org/10.1111/j.1365-2486.2008.01641.x).
- Bell RE, Banwell AF, Trusel LD and Kingslake J** (2018) Antarctic surface hydrology and impacts on ice-sheet mass balance. *Nature Climate Change* **8**(12), 1044–1052. doi: [10.1038/s41558-018-0326-3](https://doi.org/10.1038/s41558-018-0326-3).
- Carter J, Leeson A, Orr A, Kittel C and van Wessem JM** (2022) Variability in Antarctic surface climatology across regional climate models and reanalysis datasets. *Cryosphere* **16**(9), 3815–3841. doi: [10.5194/tc-16-3815-2022](https://doi.org/10.5194/tc-16-3815-2022).
- Dengler E** (2013) *Late Quaternary History of Shackleton Glacier, Antarctica*. Orono, ME: University of Maine.
- Diaz MA and 10 others** (2020) Stable isotopes of nitrate, sulfate, and carbonate in soils from the Transantarctic Mountains, Antarctica: a record of atmospheric deposition and chemical weathering. *Frontiers in Earth Science* **8**(341). doi: [10.3389/feart.2020.00341](https://doi.org/10.3389/feart.2020.00341).
- Diaz MA and 8 others** (2021a) Geochemical zones and environmental gradients for soils from the central Transantarctic Mountains, Antarctica. *Biogeosciences (Online)* **18**, 1629–1644. doi: [10.5194/bg-18-1629-2021](https://doi.org/10.5194/bg-18-1629-2021).
- Diaz MA and 7 others** (2021b) Relationship between meteoric  $^{10}\text{Be}$  and  $\text{NO}_3^-$  concentrations in soils along Shackleton Glacier, Antarctica. *Earth Surface Dynamics* **9**(5), 1363–1380. doi: [10.5194/esurf-9-1363-2021](https://doi.org/10.5194/esurf-9-1363-2021).
- Donat-Magnin M and 9 others** (2020) Interannual variability of summer surface mass balance and surface melting in the Amundsen sector, West Antarctica. *Cryosphere* **14**(1), 229–249. doi: [10.5194/TC-14-229-2020](https://doi.org/10.5194/TC-14-229-2020).
- Elliot DH, Collinson JW and Green WJ** (1996) Lakes in dry valleys at 85°S near Mount Heekin, Shackleton Glacier. *Antarctic Journal of the United States* **31**(2), 25–27.
- Gooseff MN, McKnight DM, Doran PT and Berry Lyons W** (2007) Trends in discharge and flow season timing of the Onyx River, Wright Valley, Antarctica since 1969. *US Geol. Surv. Natl. Acad. Short Res. Pap.*, USGS (OF-2007-1047). doi: [10.3133/ofr20071047SRP088](https://doi.org/10.3133/ofr20071047SRP088).
- Gooseff MN and 12 others** (2017) Decadal ecosystem response to an anomalous melt season in a polar desert in Antarctica. *Nature Ecology & Evolution* **1**, 1334–1338. doi: [10.1038/s41559-017-0253-0](https://doi.org/10.1038/s41559-017-0253-0).
- Greene CA, Gardner AS, Schlegel NJ and Fraser AD** (2022) Antarctic calving loss rivals ice-shelf thinning. *Nature* **609**(7929), 948–953. doi: [10.1038/s41586-022-05037-w](https://doi.org/10.1038/s41586-022-05037-w).
- Helsen MM, van de Wal RSW and van den Broeke MR** (2007) The isotopic composition of present-day Antarctic snow in a Lagrangian atmospheric simulation. *Journal of Climate* **20**(4), 739–756. doi: [10.1175/JCLI4027.1](https://doi.org/10.1175/JCLI4027.1).
- Jones ME and 6 others** (2019) Sixty years of widespread warming in the southern middle and high latitudes (1957–2016). *Journal of Climate* **32**(20), 6875. doi: [10.1175/JCLI-D-18-0565.1](https://doi.org/10.1175/JCLI-D-18-0565.1).
- Masson-Delmotte V and 35 others** (2008) A review of Antarctic surface snow isotopic composition: observations, atmospheric circulation, and isotopic modeling. *Journal of Climate* **21**(13), 3359–3387. doi: [10.1175/2007JCLI2139.1](https://doi.org/10.1175/2007JCLI2139.1).
- Shepherd A and 79 others** (2018) Mass balance of the Antarctic ice sheet from 1992 to 2017. *Nature* **558**(7709), 219–222. doi: [10.1038/s41586-018-0179-y](https://doi.org/10.1038/s41586-018-0179-y).
- Stokes CR, Sanderson JE, Miles BWJ, Jamieson SSR and Leeson AA** (2019) Widespread distribution of supraglacial lakes around the margin of the east Antarctic ice sheet. *Scientific Reports* **9**(1), 1–14. doi: [10.1038/s41598-019-50343-5](https://doi.org/10.1038/s41598-019-50343-5).
- Webster J, Hawes I, Downes M, Timperley M and Howard-Williams C** (1996) Evidence for regional climate change in the recent evolution of a high latitude pro-glacial lake. *Antarctic Science* **8**(1), 49–59. doi: [10.1017/S0954102096000090](https://doi.org/10.1017/S0954102096000090).
- Welch KA and 6 others** (2010) Spatial variations in the geochemistry of glacial meltwater streams in the Taylor Valley, Antarctica. *Antarctic Science* **22**(6), 662–672. doi: [10.1017/S0954102010000702](https://doi.org/10.1017/S0954102010000702).